Available online at www.sciencedirect.com
SCIENCE DIRECT®
Journal of Magnetic Resonance 172 (2005) 324–328
JMR Journal of Magnetic Resonance
www.elsevier.com/locate/jmr

A selective experiment for the sequential protein backbone assignment from 3D heteronuclear spectra

Wolfgang Bermel[a], Ivano Bertini[b,*], Isabella C. Felli[b], Roberta Pierattelli[b], Paul R. Vasos[b]

[a] *Bruker BioSpin GmbH, Rheinstetten, Germany*
[b] *CERM and Department of Chemistry, University of Florence, Sesto Fiorentino, Italy*

Received 10 August 2004; revised 21 October 2004
Available online 8 December 2005

Abstract

Two modifications of the triple-resonance CANCO sequence, designed for backbone assignment in proteins [Angew. Chem. Int. Ed. 43 (2004) 2257], are presented here. These two new sequences display the intra-residue Ca–CO correlation selectively, while in the original sequence both the inter- and the intra-residue correlations were present. In addition, one of the two variants benefits from an improved sensitivity. Both sequences are a useful complement to the CANCO sequence for facile sequence-specific protein assignment by protonless NMR.

Keywords: Protonless NMR; ^{13}C-NMR; ^{13}C-Direct detection; Sequential assignment; Protein structure

1. Introduction

The use of low-gamma nuclei detected experiments in paramagnetic molecules has been promoted as a *stand-alone* technique, thanks to the development of pulse sequences able to provide the complete assignment of backbone hetereonuclei from ^{13}C-detected experiments [1–5].

The assignment procedure consists of two steps: identifying the spin-systems based on their characteristic patterns in a CBCACO spectrum and connecting the spin systems using a CANCO and a CACO experiment [3]. The use of this approach can be profitably extended for the study of large macromolecules, as the losses of magnetization due to relaxation are minimized through the exploitation of low-gamma nuclei. In addition, the complexity of the pulse sequences is reduced by eliminating the protons from the magnetization pathway.

A problem that generally arises with the increase of the size of the proteins under investigation is resonances overlap. The CANCO sequence [3], that correlates the CO shift of one residue in the direct dimension with the ^{15}N shift of the following residue and the C$^{\alpha}$ shifts of the same and the following residue, has been conceived as a three-dimensional experiment, in which the CACO correlation experiment was expanded to the third ^{15}N dimension with the specific purpose of increasing resolution. However, as in each CACO plane the intra (C^{α}_i, CO_i) and inter (CO_i, C^{α}_{i+1}) correlations are present, in the CANCO spectrum resonance overlap can still occur.

The experiment presented here is a modification of the CANCO sequence designed to produce a 3D correlation map in which only intra-residue (C^{α}_i, CO_i) correlations are present, and these are correlated with the corresponding N_{i+1} resonance in the third dimension. This experiment is intended to complement the CANCO experiment for the identification of

* Corresponding author. Fax: +39 055 4574271.
E-mail address: bertini@cerm.unifi.it (I. Bertini).

1090-7807/$ - see front matter © 2004 Elsevier Inc. All rights reserved.
doi:10.1016/j.jmr.2004.11.005

sequential spin systems, while circumventing the overlap problem. Two pulse sequences are presented: one is more suited for comparison with the CANCO one and can be used in combination with it to generate a inter-residue selective correlation map; the second one yields an intra-residue correlation map with an enhanced signal-to-noise with respect to the original CANCO.

2. Materials and methods

2.1. Pulse sequences

The pulse sequences shown in Fig. 1 yield a $(C^{\alpha}_i, CO_i, N_{i+1})$ correlation. The initial part of the experiment is analogous to the CANCO experiment [3]. The first $\pi/2$ pulse excites the C^{α} spins. They are then evolving under the influence of their chemical shifts, of the C^{α}–C^{β} coupling which is preserved for a total period of $1/J_{C^{\alpha}C^{\beta}}$ and of the two C^{α}–N couplings to the adjacent N atoms. In contrast to the original CANCO, the C^{α}–CO coupling is also active for a $1/2J_{C^{\alpha}CO}$ period. The $\pi/2$ pulses at the end of the t_1 evolution convert the anti-phase $C^{\alpha}_y CO_z N_z$ coherence into $C^{\alpha}_z CO_z N_y$.

In the pulse sequence shown in Fig. 1A the $C^{\alpha}_z CO_z N_y$ coherence subsequently evolves under the N chemical shift in a constant-time manner and simultaneously the C^{α}–^{15}N coupling is active, so that the coherence is transformed into $CO_z N_x$. At point *c*, this is converted into $CO_y N_z$. During the last step, this coherence is then transferred into in-phase CO magnetization and subsequently detected. In the pulse sequence shown in Fig. 1B the $C^{\alpha}_z CO_z N_y$ coherence evolves under the N chemical shift in a real-time manner. At point *c*, it is converted into $C^{\alpha}_z CO_y N_z$. During the last step, this coherence evolves under the CO–N and C^{α}–CO couplings into in-phase CO magnetization which is subsequently detected.

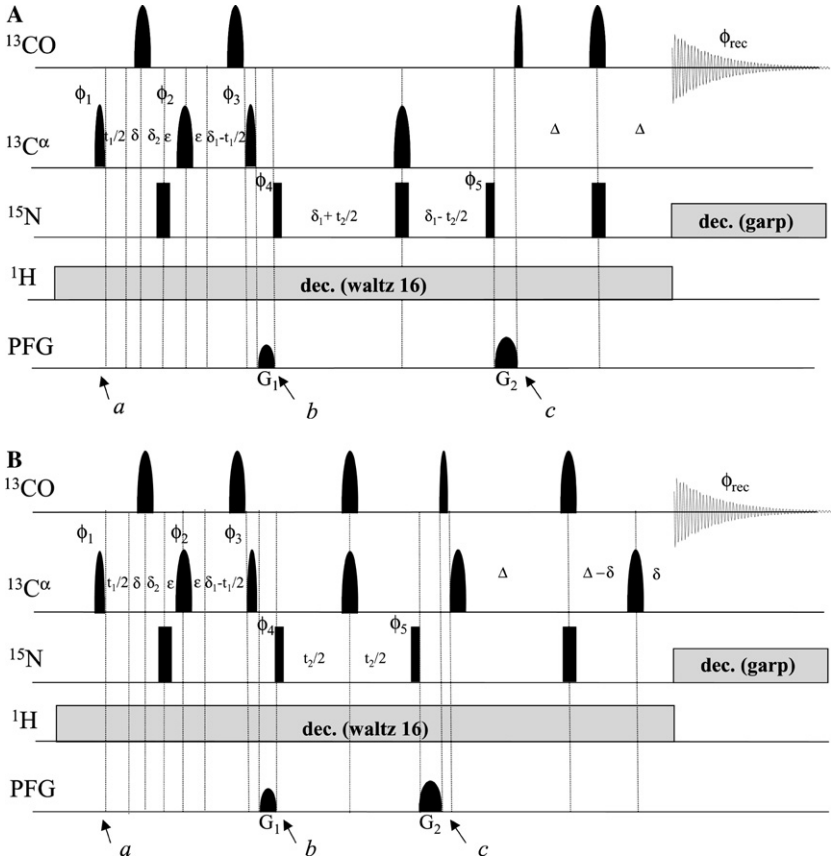

Fig. 1. 3D intra-selective CANCO pulse sequences. Narrow and wide black bars indicate non-selective $\pi/2$ and π pulses, respectively. Narrow and wide Gaussian shapes on carbon channel represent selective $\pi/2$ and π pulses, respectively. Gaussian cascades (Q3 and Q5) were used [12], 274 μs long for the $\pi/2$ pulses and 220 μs long for the π pulses. The phase cycle employed was $\phi_1 = (x, -x)$, $\phi_2 = (2x, 2(-x))$, $\phi_3 = (4x, 4(-x))$, $\phi_4 = (8x, 8(-x))$, $\phi_{rec} = (2(x, -x), 4(-x, x), 2(x, -x))$. All the pulses are applied along the *x* axis unless otherwise indicated. In the ^{15}N-refocussing sequence (A) $\phi_5 = y$ and in the CO-refocusing sequence (B) $\phi_5 = x$. The pulsed field gradients were 1.0 ms long, sine-shaped, with maximum intensities of $G_1 = 19$ G/cm and $G_2 = 16$ G/cm. The delays were $\delta_1 = \delta + \delta_2 = 11.4$ ms, $\delta = 4.4$ ms, $\varepsilon = 3.0$ ms, $\Delta = 14.2$ ms. Phase-sensitive spectra in the $^{13}C^{\alpha}(t_1)$ and $^{15}N(t_2)$ dimensions are obtained by incrementing the phases ϕ_1 and ϕ_4 in a States-TPPI manner [16].

The use of two π pulses at the C^{α} frequency during the last transfer step and of two π pulses on the CO frequency during the first transfer step ensures removal of Block–Siegert effects [6,7]. The evolution periods in the C^{α} dimension are built in a constant time (CT) manner [8].

The primary difference between the two sequences is that in the first one the NC^{α} antiphase coherence is refocused during the period in which the N magnetization is transverse while in the second one the $C^{\alpha}CON$ double antiphase is refocused during the period in which the CO magnetization is in the plane. We will thus refer to them as the ^{15}N-refocussing (Fig. 1A) and the CO-refocusing (Fig. 1B) sequence, respectively, from now on.

2.2. Sample preparation

The U-^{13}C, ^{15}N-labeled oncomodulin was expressed and purified as previously reported [9]. The protein concentration in the final NMR sample was about 2.5 mM. The sample was dissolved in a 100 mM NaCl water solution at pH 6.0 and 10% D_2O was added for the lock signal. All the spectra detailed below were recorded at 298 K.

2.3. NMR experiments

The experiments shown here were carried out on a 16.4 T Bruker Avance spectrometer operating at 700.06 MHz for ^{1}H and 176.03 MHz for ^{13}C equipped with a prototype TXO probe designed for carbon direct detected experiments. The inner coil is tuned to ^{13}C, the outer coil is double tuned to ^{1}H and ^{15}N. Composite pulse decoupling on ^{15}N was applied during the acquisition period of the experiments with an RF field strength of 0.625 kHz using Garp-4 [10] and throughout the duration of the sequences on ^{1}H with an RF field strength of 1.665 kHz (Waltz-16) [11]. The carrier frequencies for pulses applied on ^{15}N and ^{1}H were of 120.0 and 4.0 ppm, respectively.

To check sample integrity, ^{1}H–^{15}N HSQC experiments were acquired with standard parameters [12]. A CT-CACOSQ experiment was obtained using a refocused INEPT-like transfer (for transfer of magnetization from C^{α} to CO and refocusing of CO with respect to C^{α}, see Supplementary material for details on this sequence). The π/2 and π pulses were Gaussian cascades [13] 332 and 220 μs long, Q5 and Q3, respectively. The ^{13}CO–$^{13}C^{\alpha}$ spectrum was recorded with a 1.2 s recycle delay, 16 transients, and 56.5 ms acquisition time. The total acquisition time in the indirect dimension was $t_1^{\max} = 9.1$ ms. Spectral windows of 25.9 and 40.0 ppm were acquired in the ^{13}CO and $^{13}C^{\alpha}$ dimensions, respectively, corresponding to a matrix of 1024×128 complex points. The carrier on the carbon channel is set to 57.0 ppm and switched from 57.0 to 175.0 ppm before the first π/2 ^{13}CO pulse.

For the intra-selective CANCO spectra, the carrier frequencies for pulses applied on ^{13}CO, $^{13}C^{\alpha}$, ^{15}N and ^{1}H were of 175.0, 57.0, 120.0, and 5.0 ppm, respectively. Gaussian cascades (Q5 and Q3) [13] 274 μs long for the π/2-pulses and 220 μs long for the π pulses were used. For both experiments a 45.6 ms acquisition time and a 1.2 s recycle delay were used. The pulsed field gradients were 1.0 ms long, sine-shaped with maximum intensities of $G_1 = 19$ G/cm, $G_2 = 16$ G/cm. The delays were $\delta_1 = \delta + \delta_2 = 11.4$ ms, $\delta = 4.4$ ms, $\varepsilon = 3.0$ ms, and $\Delta = 14.2$ ms.

The spectra were recorded with 2k transients and 64 dummy scans. The maximum acquisition time in the indirect dimension was $t_1^{\max} = 5.7$ ms. Spectral windows of 32 and 40 ppm were acquired in the ^{13}CO and $^{13}C^{\alpha}$ dimensions, respectively. A matrix of 512×80 complex points was recorded, for a total of 52 h experimental time. Prior to Fourier transformation, expansion by linear prediction of 64 points and zero filling to 1024×512 points was applied.

3. Results and discussion

The pathways of magnetization transfer employed in the experiments designed to circumvent the use of protons differ substantially from those that are classically employed in the standard HN-based sequences [14]. The sequential correlations in protein spectra appear due to the similar magnitude of the $^{1}J_{NC^{\alpha}}$ and $^{2}J_{NC^{\alpha}}$ scalar couplings. The CANCO sequence was designed to minimize the use of $CO \rightarrow N$ and $CO \rightarrow C^{\alpha}$ transfer steps, thus reducing the periods in which CO magnetization is transverse. To preserve this feature in the selective CANCO, the approach used by Meissner and Sørensen [15] has been adopted, introducing a coupling between the C^{α} and the CO spins during the first magnetization transfer step and refocusing it during one of the subsequent steps.

One difference between the ^{15}N-refocusing sequence and the original CANCO is that it can use a slightly shorter ^{15}N constant-time evolution period, as the N–CO coupling evolution is no longer required during that delay. The CO-refocusing sequence allows one to circumvent the constant-time ^{15}N-transverse period and instead acquire real-time ^{15}N spectra, with increased sensitivity. This is due to the fact that the refocusing of the intra and inter-residue J-couplings to C^{α} is no longer required when ^{15}N is transverse but is done only when CO is transverse (see Supplementary material).

For the purpose of assignment, 3D correlation maps displaying both the intra and inter-residue signals (provided by the CANCO sequence) and only intra-residue signals (provided by the intra-selective CANCO

sequence) of comparable sensitivity are desirable. Indeed, corresponding intra-residue signals with similar shapes and intensities in the two 3D spectra may be easily identified and, eventually, the two maps can be directly subtracted. In these cases, the ^{15}N-refocussing sequence is preferable.

To compare the versatility of the assignment procedure, two-dimensional experiments were recorded using the original CANCO [3] and the two sequences described above, under the same experimental conditions, on a sample of oncomodulin, a 109 residues protein. The detected signals using the three sequences were compared on a per-residue basis, taking advantage of the available assignment [3,9].

The experiment obtained with the original CANCO sequence displayed 79% of the intra-residue correlations. Four additional intra-residue signals could be detected with the ^{15}N-refocusing sequence. The CO-refocusing sequence detects the majority of intra-correlation signals (all but three). This is the result of the increase in sensitivity due to the suppression of the period during which ^{15}N magnetization is transverse. The spectrum obtained by taking the difference between the original CANCO and the ^{15}N-refocussing selective CANCO spectra displays 92% of the inter-residue (C^{α}_{i+1}, CO_i) correlations. For the purpose of assignment, the experimental intra-selective spectrum and the inter-selective difference spectrum can be used. Selected areas of the two above mentioned spectra and the original CANCO spectrum are shown in Fig. 2.

The differences in ^{15}N transverse relaxation periods are the reason for the different number of signals detected in the three sequences. All the signals additionally detected using the ^{15}N-refocussing sequence are in potentially highly mobile regions (N- and C-termini and residue 79). They might experience conformational exchange contributions to relaxation, consequently the decrease by 5.0 ms of the ^{15}N CT period introduces a significant gain in the signal intensity.

The sequences use only pulses that covers the aliphatic region and refocussing interval of $1/J_{C^{\alpha}C^{\beta}}$, in contrast to using a more selective pulse at the C^{α} frequency. These makes the sequence longer and thus more prone to relaxation losses but avoids having to clearly discriminate the C^{α} and C^{β} region. The losses are compensated in the CO-refocusing sequence by the use of a shorter time period during which the ^{15}N magnetization is transverse.

For use with proteins in D_2O solution the proton decoupling can be switched off between points *b* and *c* and deuterium decoupling can be introduced instead. In systems where only part of the signals are affected by fast relaxation (proteins with a paramagnetic center) a refocused $H^{\alpha} \rightarrow C^{\alpha}$ INEPT transfer can be implemented at the beginning of the sequence, in order to take advantage of the $^{1}H \rightarrow {}^{13}C$ polarization transfer.

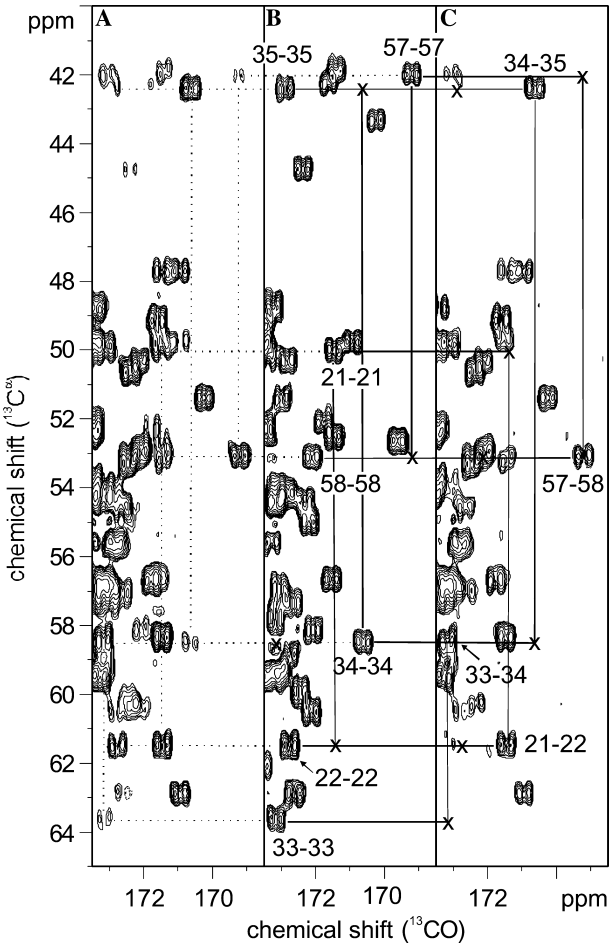

Fig. 2. Selected areas of (A) the CANCO spectrum, (B) the CO-refocussing CANCO spectrum, and (C) the difference spectrum obtained subtracting the ^{15}N-refocussing CANCO and the CANCO spectra recorded on oncomodulin at 16.4 T. The difference spectrum in (C) was obtained using the add2d command of the Bruker Xwinnmr 3.5 software without any scaling factor between the spectra. As an example, the correlations that sequentially connect residues 21–22, 33–35, and 57–58 are highlighted. In (B) and (C), where only one of the two correlations detected in CANCO is present, the black crosses indicate the position of the missing cross-peaks.

In summary, the selective-CANCO sequences presented here are a useful aid for protein backbone assignment. These sequences are an essential complement to the already available set of ^{13}C-detection based experiments for assignment of large molecular mass proteins and in all the cases where resonance broadening cannot be recovered through the TROSY approach.

Acknowledgments

We thank Prof. Harald Schwalbe for the stimulating comments on the experiments and Michael Fey (Bruker BioSpin) for the useful discussions. This work was supported in part by the EC contracts no. QLG2-CT-2002-00988 and no. HPRN-CT-2000-00092.

Appendix A. Supplementary data

Supplementary data associated with this article can be found, in the online version, at doi:10.1016/j.jmr.2004.11.005.

References

[1] F. Arnesano, L. Banci, I. Bertini, I.C. Felli, C. Luchinat, A.R. Thompsett, A strategy for the NMR characterization of type II copper(II) proteins: the case of the copper trafficking protein CopC from *Pseudomonas syringae*, J. Am. Chem. Soc. 125 (2003) 7200–7208.

[2] W. Bermel, I. Bertini, I.C. Felli, R. Kummerle, R. Pierattelli, ^{13}C direct detection experiments on the paramagnetic oxidized monomeric copper, zinc superoxide dismutase, J. Am. Chem. Soc. 125 (2003) 16423–16429.

[3] I. Bertini, L. Duma, I.C. Felli, M. Fey, C. Luchinat, R. Pierattelli, P. Vasos, A heteronuclear direct detection NMR experiment for protein backbone assignment, Angew. Chem. Int. Ed. 43 (2004) 2257–2259.

[4] T.E. Machonkin, W.M. Westler, J.L. Markley, Strategy for the study of paramagnetic proteins with slow electronic relaxation rates by NMR spectroscopy application to oxidized human [2Fe–2S]ferredoxin, J. Am. Chem. Soc. 126 (2004) 5413–5426; M. Kostic, S.S. Pochapsky, T.C. Pochapsky, Rapid recycle $^{13}C'$, ^{15}N and ^{13}C, $^{13}C'$ heteronuclear and homonuclear multiple quantum coherence detection for resonance assignments in paramagnetic proteins: example of Ni^{2+}-containing acireductome dioxygenase, J. Am. Chem. Soc. 124 (2002) 9054–9055.

[5] E. Babini, I. Bertini, F. Capozzi, I.C. Felli, M. Lelli, C. Luchinat, Direct carbon detection in paramagnetic metalloproteins to further exploit pseudocontact shift restraints, J. Am. Chem. Soc. 126 (2004) 10496–10497.

[6] F. Bloch, A. Siegert, Magnetic resonance for non rotating fields, Phys. Rev. 57 (1940) 522–527.

[7] L. Emsley, G. Bodenhausen, Phase-shifts induced by transient Bloch-Siegert effect in NMR, Chem. Phys. Lett. 168 (1990) 297–303.

[8] S. Grzesiek, A. Bax, Improved 3D triple-resonance NMR techniques applied to a 31 kDa protein, J. Magn. Reson. 96 (1992) 432–440.

[9] E. Babini, I. Bertini, F. Capozzi, C. Del Bianco, D. Holleder, T. Kiss, C. Luchinat, A. Quattrone, Solution structure of human β-parvalbumin and structural comparison with its paralog α-parvalbumin and with their rat orthologs. Biochemistry (in press).

[10] A.J. Shaka, P.B. Barker, R. Freeman, Computer-optimized decoupling scheme for wideband applications and low-level operation, J. Magn. Reson. 64 (1985) 547–552.

[11] A.J. Shaka, J. Keeler, R. Freeman, Evaluation of a new broadband decoupling sequence: WALTZ-16, J. Magn. Reson. 53 (1983) 313–340.

[12] L.E. Kay, P. Keifer, T. Saarinen, Pure absorption gradient enhanced heteronuclear single quantum correlation spectroscopy with improved sensitivity, J. Am. Chem. Soc. 114 (1992) 10663–10665.

[13] L. Emsley, G. Bodenhausen, Gaussian pulse cascades: new analytical functions for rectangular selective inversion and in-phase excitation in NMR, Chem. Phys. Lett. 165 (1990) 469–476.

[14] L.E. Kay, M. Ikura, R. Tschudin, A. Bax, Three-dimensional triple-resonance NMR spectroscopy of isotopically enriched proteins, J. Magn. Reson. 89 (1990) 496–514.

[15] A. Meissner, O.W. Sørensen, A sequential HNCA NMR pulse sequence for protein backbone assignment, J. Magn. Reson. 150 (2001) 100–104.

[16] D. Marion, M. Ikura, R. Tschudin, A. Bax, Rapid recording of 2D NMR spectra without phase cycling. Application to the study of hydrogen exchange in proteins, J. Magn. Reson. 85 (1989) 393–399.